Human Absorbed Dose Estimation of [113mIn] In-PSMA-617 for Prostate Cancer Imaging Using Animal Data and Monte Carlo Simulation

Leyla Akbari (MSc)[1], Samaneh Zolghadri (PhD)[2]*, Arezou Karimian (PhD Candidate)[2], Hassan Yousefnia (PhD)[2], Saeed Ranjbar (MSc)[2]

[1]Department of Radiation Application, School of Mechanical Engineering, Shiraz University, Shiraz, Iran
[2]Radiation Application Research School, Nuclear Science and Technology Research Institute (NSTRI), Tehran, Iran

ABSTRACT

Background: Prostate Cancer (PC) is the second leading cause of cancer death in men, and early diagnosis is essential since localized PC is curable. International Commission on Radiological Protection (ICRP) and Medical Internal Radiation Dose (MIRD) guidelines should be followed to guarantee accurate and reliable dosimetry evaluations.

Objective: In this study, the radiation absorbed dose of the human organs of [113mIn] In-PSMA-617 was estimated using animal data and Monte Carlo simulation in Oak Ridge National Laboratory (ORNL) human phantom to evaluate the dosimetry of a novel Single Photon Emission Computed Tomography (SPECT) agent.

Material and Methods: In this experimental study, the radiolabeled compound was prepared at optimized conditions, and its biodistribution was studied at different intervals. The absorbed dose of human organs was calculated by MCNPX software by tracking a total of 10^6 particles for a gamma of 391.7 keV.

Results: The biodistribution of the radiotracer in animals showed the activity was removed from the blood circulation very fast, and significant uptake was observed in the kidneys and the PSMA-expressing organs. The kidneys received the highest absorbed dose with 9 ±1 µGy/MBq.

Conclusion: This agent shows the potential of [113mIn] In-PSMA-617 for prostate cancer imaging, particularly in regions with limited access to Positron Emission Tomography (PET) imaging. The generator-based production of [113m]In allows for widespread availability, making it a practical alternative to other PSMA-based radiopharmaceuticals. Additionally, the low radiation burden and efficient renal clearance support its safety for repeated imaging.

Introduction

After lung cancer, Prostate Cancer (PC) is the most common cause of death for males globally [1]. Recent projections estimate approximately 299010 new prostate cancer cases and 35250 deaths in the United States for 2024, underscoring its significant public health

*Corresponding author:
Samaneh Zolghadri
Radiation Application Research School, Nuclear Science and Technology Research Institute (NSTRI), Tehran, Iran
E-mail:
szolghadri@aeoi.org.ir

impact [2]. The timely diagnosis of PC helps to decide better follow-up and clinical treatment implementation [3]. An accurate diagnosis of PC allows for treatment before it spreads in the body. The regional PC treatment has a 100% cure rate, whereas metastatic PC has a 30% survival rate after 5 years [4,5].

Prostate-Specific Membrane Antigen (PSMA) is a transmembrane glycoprotein expressed in over 90% of PC cells, with its upregulation closely associated with tumor progression and invasiveness. It is localized on the surface of various tumor types, particularly prostate carcinoma.

This makes PSMA an ideal target for diagnosing and treating PC [6-8], and its function is as a glutamate-preferring carboxypeptidase [9,10]. PSMA-617 is designed as a small peptide that binds to this protein and enables the delivery of therapeutic and imaging radionuclides to cancer cells. Radioactive compounds, such as ^{68}Ga [11], ^{89}Zr [12], ^{64}Cu [13], ^{225}Ac [14], ^{90}Y [15], ^{213}Bi [16], ^{44}Sc, ^{177}Lu [17], and ^{111}In [18] bind to PSMA-617, and depending on the type of radionuclide; they are also used in Positron Emission Tomography (PET), and Single Photon Emission Computed Tomography (SPECT) imaging or cancer treatment [11,19]. Among the diagnostic radionuclides used in SPECT imaging, ^{99m}Tc is the most widely employed due to its good physical qualities and easy availability via the ^{99}Mo/^{99m}Tc generator. However, shortages of this necessary radionuclide have been recently reported. To compensate for this shortcoming, research was devoted to the development of novel radionuclides. Meanwhile, Carrier-free ^{113m}In and its radiolabeled compounds have been introduced for imaging of the body, brain, lungs, Gastrin-Releasing Peptide Receptors (GRPR)-expressing and neuroendocrine tumors because of its short half-life (1.7 h), gamma of 391.7 keV, and intensity of 64.2% [20-22]. In addition to the unique properties of this radionuclide, its radiolabeling chemistry is straightforward and available in a generator-based system [23].

In nuclear medicine, dosimetry is used to assess the radiation absorbed dose by patients. When licensing new radiopharmaceuticals, the U.S. Food and Drug Administration (FDA) and Emergency Medical Assistance (EMA) require dosimetry tests to assess radiation exposure to key organs and body parts, thereby reducing possible hazards. Furthermore, pharmacokinetics and biodistribution evaluations help clinicians make educated judgments, and adhering to International Commission on Radiological Protection (ICRP) and Medical Internal Radiation Dose (MIRD) guidelines ensures that these assessments are accurate and dependable [24]. Therefore, the accumulated activity and absorbed dose of organs after injection of [^{113m}In] In-PSMA-617 should be considered before using the complex as a radiopharmaceutical in clinical applications [25].

The MIRD methodology is a widely used approach for estimating radiation doses in nuclear medicine and plays a crucial role in evaluating the safety and effectiveness of radiopharmaceuticals [26]. This method provides a systematic framework for calculating absorbed dose by determining the Specific Absorbed Fractions (SAFs), which represent the fraction of energy emitted by a radionuclide that is absorbed by target organs [27]. In this study, the MIRD approach, combined with Monte Carlo simulations, was used to estimate the absorbed dose of [^{113m}In] In-PSMA-617 in different human organs. The Sparks et al. method was utilized to extrapolate activity accumulation from animal models to humans, ensuring a reliable dosimetric assessment [28]. SAF values were calculated using computational phantoms, such as the Oak Ridge National Laboratory (ORNL) phantom, along with Monte Carlo transport codes like Monte Carlo N-Particle (MCNP) [25,29]. Since high radiation doses to non-target organs remain a major limitation of existing PSMA-based agents, accurate dosimetry is essential to assess whether

[^{113m}In] In-PSMA-617 offers a safer alternative with lower absorbed doses. This analysis provides critical data for supporting its potential clinical application in prostate cancer imaging.

The field of nuclear medicine is actively researching various radiolabeled agents for potential use in diagnostic imaging and radionuclide therapy, and a great amount of human data is also needed. To minimize human radiation exposure, it is essential to conduct predictive dosimetry studies based on *in vivo* biokinetics to estimate absorbed doses in humans from animal data and expedite the development of radioactive compounds for clinical experiments. This preliminary step is in accordance with ICRP guidelines, which recommend conducting preclinical evaluations before proceeding to human studies involving a limited number of volunteers [30,31]. While radiation dosimetry is not typically part of diagnostic tests, understanding the absorbed doses in critical organs, such as bone marrow, liver, kidney, spleen, etc., is pivotal for determining the maximum injecting activity and comprehending dose-response relationships for toxicities [32].

Existing PSMA-based radiopharmaceuticals, such as ^{68}Ga-PSMA-11 and ^{99m}Tc-HYN-IC-PSMA, face limitations that justify the need for exploring alternative agents. A key concern is the high radiation dose absorbed by organs, which may increase potential toxicity risks, especially in repeated imaging scenarios. Additionally, the limited availability of radionuclides like ^{68}Ga, which depends on costly and regionally restricted generators, presents logistical challenges. In contrast, [^{113m}In] In-PSMA-617 delivers a lower absorbed radiation dose and can be conveniently produced using a generator system, positioning it as a promising alternative for wider clinical use. This study aimed to further investigate [^{113m}In] In-PSMA-617. Dosimetry profile to support its potential use in PC imaging. In this study, the SAFs and S-values for different source and target organs for ^{113m}In radionuclide, and

absorbed dose of different human organs after injection of [^{113m}In] In-PSMA-617 were calculated using the MIRD methodology and Monte Carlo simulations.

Material and Methods

This is an experimental study.

Preparation, quality control, and Biodistribution studies of [^{113m}In] In-PSMA-617

The ^{113}Sn/^{113m}In generator was prepared by irradiating natural indium with 30 MeV protons to produce ^{113}Sn, which was then loaded onto a zirconium chloride column. ^{113m}In was eluted from the generator by 0.05 M Hydrochloric acid (HCl) in the form of [^{113m}In] InCl$_3$. The radionuclide purity of ^{113m}In was assessed using an High Purity Germanium (HPGe) detector. The chemical purity of the solvent was measured by Inductively Coupled Plasma Mass (ICP-MS) spectrometry, and radiochemical purity was determined by Radio-Thin Layer Chromatography (RTLC) method. Radiolabeling conditions for the PSMA-617 peptide with ^{113m}In were optimized by adjusting temperature, pH, ligand concentration, and reaction time. RTLC and High-Performance Liquid Chromatography (HPLC) were used to assess radiochemical purity. [^{113m}In] In-PSMA-617 (5.55 MBq; 200 μL) was injected into 18-week-old rats. Biodistribution of the complex was assessed in rat organs at various intervals (15-120 min), along with washing and weighing tissues to calculate the percentage Injected Dose (ID) per gram of tissue (%ID/g) according to Equation 1. Biodistribution refers to the distribution and accumulation of the radiolabeled compound in tissues and organs, which can indicate what percentage of the injected dose is absorbed by each organ. This information is crucial for evaluating the efficacy and safety [^{113m}In] In-PSMA-617 in the body and predicting how it will be distributed in the human body. The injected activity is not corrected for decay and the mass of each organ.

$$\%ID = \frac{A}{\text{injected activity} \times \text{Tissue weight}_{(g)}} \times 100 \quad (1)$$

Where, A is the activity measured in the tissue [22-23]. This study was approved by Nuclear Science and Technology Research Institute (NSTRI) Ethical Committee.

S-value calculations

The ORNL worked on practical dosimetry applications for the MIRD from 1970 to 1980. In 1987, Cristy and Eckerman developed the ORNL phantom (Figure 1), which includes simplified human body models of varying ages using shapes like elliptical cylinders and cones [33]. This model features various organs and tissues, such as the urinary bladder mucosa, respiratory airways, colon, salivary glands, kidneys, head, and brain, with mass densities and compositions based on ICRP and International Commission on Radiation Units and Measurements (ICRU) publications [34].

MCNP simulates the transportation of particles like photons and electrons in organs. It can calculate SAFs and uses various tallies, including F6 (absorbed dose from energy deposition), F4 (photon flux converted to absorbed dose), and F8 (deposited energy from secondary particles). These methods allow for an estimation of absorbed dose through three different approaches [28, 35].

In this study, SAFs and S-values were calculated by MCNPX in the ORNL adult male phantom [33]. Sources were distributed uniformly in each source of the organs and were identified with the Visual Editor-VISD Version X_22S, which operates on a Cartesian coordinate system. The F6 TALLY was employed, and all output results were provided in MeV/g. To determine energy and decay probability while minimizing errors to less than 5%, a total of 10^6 particles were transported. The calculations were done without considering the energy cutoff. Finally, the SAFs were then used to calculate the S-values for each source and target organ. To verify the Monte Carlo simulation, the calculated S-values were compared with those in OLINDA/EXM software [36, 37]. OLINDA/EXM is a standard software for nuclear medicine dosimetry, calculating absorbed dose and S-value based on MIRD models and biokinetic data using standard phantoms.
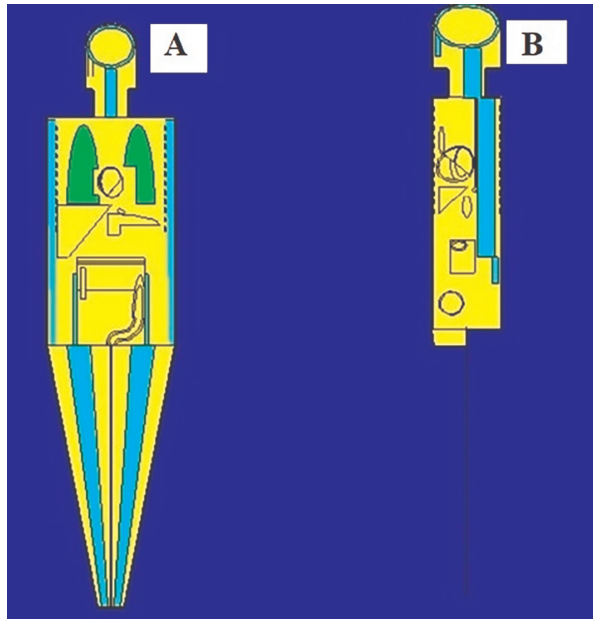
Accumulated activities of human organs

To estimate the human absorbed dose, the method outlined by Sparks et al. (Eq.2) was used to extrapolate the accumulated activity in animals to humans [28].

$$\bar{A}_{\text{Human organ}} = \bar{A}_{\text{Animal organ}} \times \frac{\text{Organ mass}_{\text{Human}} / \text{Body mass}_{\text{Human}}}{\text{Organ mass}_{\text{Animal}} / \text{Body mass}_{\text{Animal}}} \quad (2)$$

The quantity $\tilde{A}$ represents the accumulated activity within the source organ, and it is calculated using Eq. 3.

$$\tilde{A} = \int_0^\infty A(t)\,dt \quad (3)$$

The activity of each organ at time (t) is denoted as A(t).

The accumulated activity of the animal source organ was calculated by graphing the percentage of the injected dose over time and calculating the area under the curves. The

Figure 1: Oak Ridge National Laboratory (ORNL) human phantom in A) Coronal & B) Sagittal forms.

curves were extended to infinity by matching the end of each curve to a mono-exponential curve with an exponential coefficient equal to the physical decay constant of [113mIn]. To estimate the accumulated activity in humans, the average weight of each organ was applied to a typical human. Also, the organ mass of the injected mice was used as the animal organ mass.

Human absorbed dose

The MIRD method was used to calculate the absorbed dose for each human organ, employing Eq. 4.

$$\tilde{D}(r_k) = \sum_h \tilde{A} S(r_k \leftarrow r_h) \qquad (4)$$

$\tilde{D}(r_k)$ represents the absorbed dose in the organ, and $\tilde{A}_h$ is the accumulated activity in the source organs. $S(r_k \leftarrow r_h)$ is influenced by the physical decay properties of the radionuclides, the organ size, and the range of the emitted radiations [37].

Results

Preparation, quality control, and Biodistribution studies of [113mIn] In-PSMA-617

[113mIn] InCl$_3$, with a radionuclide purity greater than 99.99%, containing less than 0.1 ppm of potential metal ion impurities, such as iron, zinc, copper, zirconium, and tin. A radiochemical purity exceeding 99% was achieved and used for labeling purposes. The radiochemical purity of more than 99% was used for labeling purposes. [113mIn] In-PSMA-617 radiolabeled compound was prepared at optimized conditions (pH=3, temperature =95 °C, time=10 min, amount of peptide =14.6 nmol) with radiochemical purity >99% (Figure 2), and specific activity >4.9 TBq/mmol. HPLC analysis revealed that free indium with a more hydrophilic nature, is washed more quickly (3.93 min), while the radiolabeled compound is washed after 15.54 min.

The biodistribution of radiolabeled compound in animal organs was demonstrated for up to 120 min by non-decay corrected curves (Figure 3). It can be perceived that the concentration of the substance in almost all the organs decreased with time. [113mIn] In-PSMA-617 exhibited the highest uptake in the kidneys (6.42% at 15 min), confirming renal excretion as the primary clearance route, with levels decreasing over time. Liver and spleen retention were minimal, indicating low hepatobiliary excretion and reduced interaction with the reticuloendothelial system.
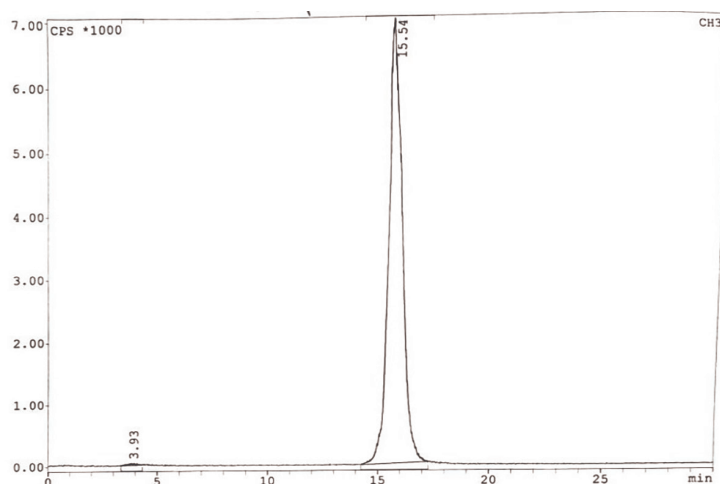

Figure 2: High Performance Liquid Chromatography (HPLC) chromatogram of [113mIn] In-PSMA-617 radiolabeled compound. Free indium with a more hydrophilic nature, is washed more quickly, while [113mIn] In-PSMA-617 is washed later.

Calculation of S-values and absorbed dose

The comparison of S-values, calculated in this study, and those from OLINDA software showed the difference below 5%, which confirmed the simulation (Table 1). The S-values for [113mIn] radionuclide were calculated on the human ORNL phantom. Finally, the human absorbed dose after injection of [113mIn] In-PSMA-617 was estimated according to the animal biodistribution data (Table 2).

According to the comparison of PSMA-based diagnostic radiopharmaceuticals (Table 3), [113mIn] In-PSMA-617 leaves a much lower absorbed dose in the organs compared to other radiolabeled PSMA compounds and ICRP safety limits. This is because the dose received by the organs (Eq. 3), is greatly affected by the physical properties of the radionuclide contained in a radiolabeled
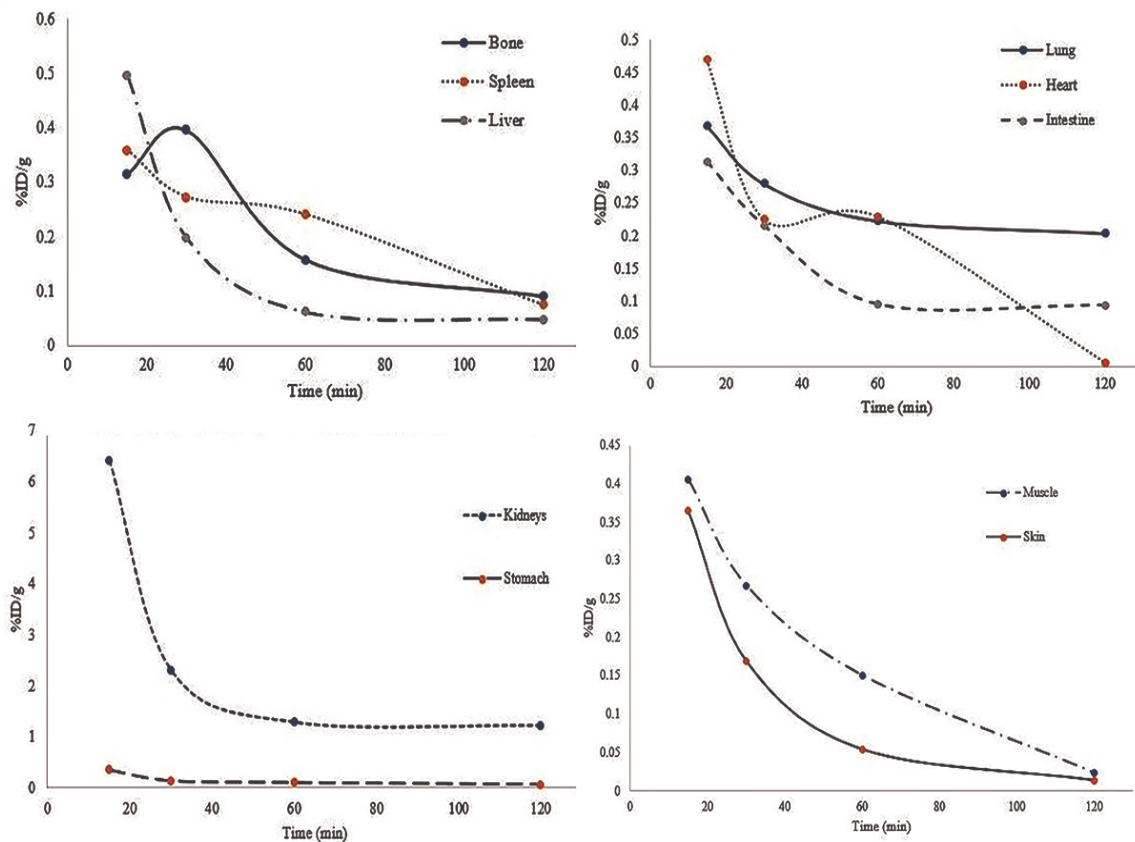
Figure 3: Non-decay corrected curve of [113mIn] In-PSMA-617 in different time points in rats. The highest uptake in the kidneys confirmed renal excretion of the complex as the primary clearance route. (PSMA: Prostate-Specific Membrane Antigen)

Table 1: Comparisons of S values calculated with MCNPX 2.7 and OLINDA for [113mIn]

Source Organ		Kidneys				
Target Organ		Heart	Kidneys	Liver	Spleen	Stomach
S values (mGy/MBq.s)	OLINDA	1.503E-7	9.913E-6	5.376E-7	1.222E-6	4.716E-7
	This study	8.435E-7	9.144E-6	4.976E-7	1.100E-6	4.294E-7

Table 2: Estimation of human equivalent dose in Microgray/MegaBecquerel (µGy/MBq) and human effective dose in MicroSievert/MegaBecquerel (µSv/MBq) after injection of [^{113m}In] In-PSMA-617. (PSMA: Prostate-Specific Membrane Antigen)

Target organs	Equivalent dose (µGy/MBq)	*Weighting factor	Effective dose (µSv/MBq)
Pancreas	0.6±0.1	0.008	0.005
Urinary Bladder Wall	0.6±0.0	0.04	0.024
Skin	0.2±0.0	0.01	0.002
Adrenals	0.6±0.1	0.008	0.005
Heart Wall	0.8±0.0	0.008	0.006
Muscle	0.4±0.0	0.008	0.003
Red Marrow	0.5±0.0	0.12	0.060
Gallbladder Wall	0.8 ±0.1	0.008	0.006
Small Intestine	1.1 ±0.1	0.008	0.009
Stomach	0.5 ±0.0	0.12	0.060
Thyroid	0.3±0.0	0.04	0.012
Bone Surfaces	0.4±0.0	0.01	0.004
Brain	0.1±0.0	0.01	0.001
Kidneys	9±1	0.008	0.072
Spleen	0.7±0.1	0.008	0.006
Liver	5±1	0.04	0.200
Lungs	0.4±0.0	0.12	0.048
Total Body	0.4±0.0		0.523

*Based on ICRP 103

Discussion

Extrapolating animal data to humans has limitations, primarily due to potential differences in drug pharmacokinetics, including organ absorption and clearance timing. These variations can exist not only between species but also between individuals. Such differences may lead to over- or underestimation of the absorbed dose in human organs. Despite these challenges, animal studies remain an accepted initial step in estimating human dosimetry.

Although physiological and metabolic differences exist between species, such as mice and humans, and even among individual humans, these variations can influence the biodistribution, metabolism, and clearance of radiopharmaceuticals. Nevertheless, estimating human organ absorbed doses based on animal biodistribution data remains a crucial preliminary step in the development of new radiopharmaceuticals [42]. Several methods for extrapolating organ uptake from animals to humans have been proposed by Sparks et al. [28], including no extrapolation, relative organ mass extrapolation, physiological time extrapolation, and a combination of mass and time-based methods. In this study, the relative organ mass extrapolation method was employed. While the relative organ mass extrapolation method assumes a proportional correlation in organ uptake between species and does not fully account for interspecies differences in metabolic and physiological parameters, it

compound, and also the effective half-life of the radiotracer (Table 4).

remains a well-established approach for initial dosimetric evaluations and risk assessment. This methodology is consistent with ICRP Publication 62 recommendations [43], and serves as a critical tool for guiding the progression to human trials. Future studies will aim to validate these extrapolated estimates through comparisons with human clinical data and published results from similar radiopharmaceuticals, thereby further refining the accuracy and clinical applicability of the absorbed dose estimations.

Table 3: Comparison of the human absorbed dose (mGy/185 MBq) for ^{68}Ga-PSMA-11, ^{99m}Tc-HYNIC-PSMA, [^{44}Sc] Sc-PSMA-617, and [^{113m}In] In-PSMA-617. (PSMA: Prostate-Specific Membrane Antigen)

Target organs	^{68}Ga-PSMA-11	^{99m}Tc-HYNIC-PSMA	[^{44}Sc]Sc-PSMA-617	[^{113m}In] In-PSMA-617
Urinary Bladder Wall	15.5	6.53	41.4	1.34
Liver	5.44	6.96	19.8	0.92
Adrenals	1.48	0.53	14.1	0.11
Gallbladder Wall	1.36	0.48	8.68	0.14
Brain	0.59	0.08	3.18	0.02
Lungs	0.08	1.00	4.42	0.08
Spleen	0.07	1.24	34.2	0.13
Small Intestine	1.00	0.35	10.2	0.20
Heart Wall	0.84	0.72	5.07	0.14
Bone Surfaces	1.89	0.44	4.68	0.08
Stomach	0.97	0.30	5.49	0.10
Kidneys	45.5	5.31	59.0	1.67
Muscle	0.78	0.24	-	0.07
Red Marrow	2.22	0.23	6.12	0.10
Pancreas	1.32	0.46	6.25	0.11
Total Body	1.14	0.29	14.0	0.07
Reference	[38]	[39]	[40]	This study

PSMA: Prostate-Specific Membrane Antigen

Table 4: Comparison of physical properties of some diagnostic radionuclides.

Radionuclides	^{68}Ga	^{99m}Tc	^{44}Sc	^{113m}In
Half-Life (min)	67	360	240	99
Decay mode	β+	IT	β+	IT
$E_{\beta+(keV)}$ (Intensity)	836 (87%) 352 (1.19%)	-	630.2 (94%)	-
$E_{\gamma(keV)}$ (Intensity)	1077.34 (3.22%) 1883.16 (0.137%)	140.511 (89%)	1157.02 (99.887%)	391.69 (64.94%)
Production (Availability)	Cyclotron (Generator)	Reactor (Generator)	Cyclotron (Cyclotron)	Cyclotron (Generator)
Reference		[41]		

In the present study, the biodistribution of radiopharmaceuticals in rats was determined and extrapolated to humans based on the accepted procedures. Furthermore, it is necessary to abide by the maximum allowed values of the absorbed doses of a radiation source in different organs as defined by the regulations [37]. The computations suggest that the absorbed doses in every organ are within the allowed level, it may be effective as a diagnostic agent. For better understanding, the absorbed dose received by human organs after injection of 185 MBq [^{113m}In] In-PSMA-617 was compared with other PSMA-based diagnostic agents (Table 2).

A comparison of the physical properties of diagnostic radionuclides, ^{68}Ga, ^{99m}Tc, ^{44}Sc, and ^{113m}In, shows that ^{113m}In has several advantages. It has a shorter physical half-life than both ^{99m}Tc and ^{44}Sc, which contributes to a reduced effective half-life of the labeled compound. Additionally, unlike ^{68}Ga and ^{44}Sc, ^{113m}In does not emit any particulate radiation, potentially lowering radiation dose to non-target tissues. Based on the information in Tables 2 and 3, [^{113m}In] In-PSMA-617, as promising radiotracer for clinical SPECT imaging, is a safe imaging agent, due to its special physical characteristics, low human absorbed dose, and availability in the form of ^{113}Sn/^{113m}In generator.

This research provides important dosimetric insights into [^{113m}In] In-PSMA-617, but several limitations should be noted. The use of animal biodistribution data may not fully capture human pharmacokinetics due to differences in organ size, blood flow, and receptor expression. The Monte Carlo simulations, though validated, assume homogeneous activity distribution, which may not reflect biological variability. Additionally, patient-specific factors, such as renal function and disease progression, were not considered, potentially affecting radiotracer clearance. While [^{113m}In] In-PSMA-617 shows a low radiation burden, further clinical trials are needed to confirm

its safety, efficacy, and diagnostic accuracy in prostate cancer patients. Human studies will be essential to refine dosimetric models and support clinical implementation.

This study pioneers the dosimetry evaluation of [^{113m}In] In-PSMA-617, demonstrating its feasibility as a new SPECT imaging agent for prostate cancer. The combination of lower radiation dose, generator-based availability, and safety validation via Monte Carlo simulations sets it apart as a promising candidate for clinical application. [^{113m}In] In-PSMA-617 has significant potential for clinical applications, especially in remote nuclear medicine centers. Its generator-based production using the long-lived ^{113}Sn/^{113m}In generator makes it highly accessible, cost-effective, and easier to distribute compared to other radiopharmaceuticals. This advantage is particularly important in regions with limited access to advanced facilities. In addition, [^{113m}In] In-PSMA-617 offers low radiation exposure to human organs and demonstrates efficient renal clearance. These features make it a promising diagnostic agent for SPECT imaging of prostate cancer, especially in settings where PET is not available.

Conclusion

[^{113m}In] In-PSMA-617 demonstrates significant promise as a safe and effective radiopharmaceutical for SPECT imaging of prostate cancer, especially in remote nuclear medicine centers due to its generator-based production. The low radiation burden to human organs, favorable biodistribution profile, and ease of production make it a compelling alternative to existing PSMA-based imaging agents. The Monte Carlo simulations and dosimetric evaluations have shown that the absorbed dose from this agent is well within acceptable safety limits, further supporting its clinical potential. However, these results are promising, further studies, particularly clinical trials, are needed to validate the dosimetry findings in human subjects. These trials will be crucial to confirm the safety, efficacy, and optimal

clinical application of [^{113m}In] In-PSMA-617 in prostate cancer imaging and to ensure its broader use in clinical practice.

Authors' Contribution

L. Akbari performed the main experimental parts of the study. S. Zolghadri and H. Yousefnia conducted the main parts of the study and analyzed the data. S. Zolghadri wrote the main manuscript text. A. Karimian and S. Ranjbar performed dosimetry calculations and helped in different parts of the study. All authors reviewed and approved the manuscript.

Ethical Approval

This study was approved by NSTRI Ethical Committee with approval No. RA-0-MP-0110-17.

Funding

None

Conflict of Interest

None

References

1. Clancy E. ACS Report Shows Prostate Cancer on the Rise, Cervical Cancer on the Decline. Renal & Urology News; UCONN; 2023.

2. Siegel RL, Giaquinto AN, Jemal A. Cancer statistics, 2024. *CA Cancer J Clin.* 2024;**74**(1):12-49. doi: 10.3322/caac.21820. PubMed PMID: 38230766.

3. Wei JT, Barocas D, Carlsson S, Coakley F, Eggener S, Etzioni R, et al. Early Detection of Prostate Cancer: AUA/SUO Guideline Part I: Prostate Cancer Screening. *J Urol.* 2023;**210**(1):46-53. doi: 10.1097/JU.0000000000003491. PubMed PMID: 37096582. PubMed PMCID: PMC11060750.

4. Sharifi M, Yousefnia H, Bahrami-Samani A, Jalilian AR, Zolghadri S, Alirezapour B, et al. Optimized production, quality control, biological evaluation and PET/CT imaging of 68Ga-PSMA-617 in breast adenocarcinoma model. *Radiochimica Acta.* 2017;**105**(5):399-407. doi: 10.1515/ract-2016-2632.

5. American Cancer Society. Key Statistics for Prostate Cancer. 2024. Available From: https://www.cancer.net/cancer-types/prostate-cancer/statistics.

6. Van Der Sar EC, Van Kalmthout LM, Lam MG. PSMA PET/CT in de diagnostiek van primaire prostaatkanker: een samenvatting van de huidige literatuur. *Tijdschr Urol.* 2020;**10**(6-7):101-8. doi: 10.1007/s13629-020-00297-5.

7. Ross JS, Sheehan CE, Fisher HA, Kaufman RP Jr, Kaur P, Gray K, et al, Correlation of primary tumor prostate-specific membrane antigen expression with disease recurrence in prostate cancer. *Clin Cancer Res.* 2003;**9**(17):6357-62. PubMed PMID: 14695135.

8. Troyer JK, Beckett ML, Wright GL Jr. Detection and characterization of the prostate-specific membrane antigen (PSMA) in tissue extracts and body fluids. *Int J Cancer.* 1995;**62**(5):552-8. doi: 10.1002/ijc.2910620511. PubMed PMID: 7665226.

9. O'Keefe DS, Su SL, Bacich DJ, Horiguchi Y, Luo Y, Powell CT, et al. Mapping, genomic organization and promoter analysis of the human prostate-specific membrane antigen gene. *Biochim Biophys Acta.* 1998;**1443**(1-2):113-27. doi: 10.1016/s0167-4781(98)00200-0. PubMed PMID: 9838072.

10. Pinto JT, Suffoletto BP, Berzin TM, Qiao CH, Lin S, Tong WP, et al. Prostate-specific membrane antigen: a novel folate hydrolase in human prostatic carcinoma cells. *Clin Cancer Res.* 1996;**2**(9):1445-51. PubMed PMID: 9816319.

11. Liu C, Liu T, Zhang N, Liu Y, Li N, Du P, et al. 68Ga-PSMA-617 PET/CT: a promising new technique for predicting risk stratification and metastatic risk of prostate cancer patients. *Eur J Nucl Med Mol Imaging.* 2018;**45**(11):1852-61. doi: 10.1007/s00259-018-4037-9. PubMed PMID: 29717333.

12. Rosar F, Schaefer-Schuler A, Bartholomä M, Maus S, Petto S, Burgard C, et al. [89Zr]Zr-PSMA-617 PET/CT in biochemical recurrence of prostate cancer: first clinical experience from a pilot study including biodistribution and dose estimates. *Eur J Nucl Med Mol Imaging.* 2022;**49**(13):4736-47. doi: 10.1007/s00259-022-05925-3. PubMed PMID: 35930033. PubMed PMCID: PMC9606102.

13. Grubmüller B, Baum RP, Capasso E, Singh A, Ahmadi Y, Knoll P, et al. 64Cu-PSMA-617 PET/CT Imaging of Prostate Adenocarcinoma: First In-Human Studies. *Cancer Biother Radiopharm.* 2016;**31**(8):277-86. doi: 10.1089/cbr.2015.1964. PubMed PMID: 27715146.

14. Kratochwil C, Bruchertseifer F, Giesel FL, Weis M, Verburg FA, Mottaghy F, et al. 225Ac-PSMA-617 for PSMA-Targeted α-Radiation Therapy of Metastatic Castration-Resistant Prostate Cancer. *J Nucl Med.* 2016;**57**(12):1941-4. doi: 10.2967/

jnumed.116.178673. PubMed PMID: 27390158.

15. Rathke H, Flechsig P, Mier W, Bronzel M, Mavriopoulou E, Hohenfellner M, et al. Dosimetry Estimate and Initial Clinical Experience with 90Y-PSMA-617. *J Nucl Med.* 2019;**60**(6):806-11. doi: 10.2967/jnumed.118.218917. PubMed PMID: 30389816.

16. Kratochwil C, Schmidt K, Afshar-Oromieh A, Bruchertseifer F, Rathke H, Morgenstern A, et al. Targeted alpha therapy of mCRPC: Dosimetry estimate of 213Bismuth-PSMA-617. *Eur J Nucl Med Mol Imaging.* 2018;**45**(1):31-7. doi: 10.1007/s00259-017-3817-y. PubMed PMID: 28891033. PubMed PMCID: PMC5700223.

17. Sinnes JP, Bauder-Wüst U, Schäfer M, Moon ES, Kopka K, Rösch F. 68Ga, 44Sc and 177Lu-labeled AAZTA5-PSMA-617: synthesis, radiolabeling, stability and cell binding compared to DOTA-PSMA-617 analogues. *EJNMMI Radiopharm Chem.* 2020;**5**(1):28. doi: 10.1186/s41181-020-00107-8. PubMed PMID: 33242189. PubMed PMCID: PMC7691401.

18. Schollhammer R, De Clermont Gallerande H, Yacoub M, Quintyn Ranty ML, Barthe N, Vimont D, et al. Comparison of the radiolabeled PSMA-inhibitor 111In-PSMA-617 and the radiolabeled GRP-R antagonist 111In-RM2 in primary prostate cancer samples. *EJNMMI Res.* 2019;**9**(1):52. doi: 10.1186/s13550-019-0517-6. PubMed PMID: 31161459. PubMed PMCID: PMC6546761.

19. Akbari L, Sina S, Zolghadri S, Moghaddasi A, Hadad K, Yousefnia H. [113mIn] In-PSMA: high potential agent for SPECT imaging of prostate cancer. *Radiochimica Acta.* 2024;**112**(11):883-94. doi: 10.1515/ract-2024-0298.

20. Ranjbar S, Aghamiri SMR, Rajabifar S, Zolghadri S, Yousefnia H. [113mIn]In-RM2: a high potential agent for SPECT imaging of GRPR-expressing tumors. *Phys Eng Sci Med.* 2025;**48**(1):273-83. doi: 10.1007/s13246-024-01510-0. PubMed PMID: 39760843.

21. Moazami-Ashtiani M, Rajabifar S, Zolghadri S, Yousefnia H. [113mIn]In-AMBA: A Novel Diagnostic Agent for SPECT Imaging of GRPR-Expressing Tumors. *Nucl Med Mol Imaging.* 2025;**59**(2):125-134. doi: 10.1007/s13139-025-00906-4. PubMed PMID: 40125027. PubMed PMCID: PMC11923307.

22. Bolourinovin F, Mirzaei M, Faghihi R, Joharidaha F, Sina S, Hadad K, et al. Preparation, Quality control, Biodistribution of [113mIn] In-DOTATATE. *Journal of Nuclear Science, Engineering and Technology.* 2024;**45**(3):29-35. doi: 10.24200/nst.2024.1526.

23. Bolorinovin F, Mirzaei M, Faghihi R, Joharidaha F, Sina S, Hadad K, Yousefnia H. Design and construction of a 113Sn/113mIn generator using irradiation of natural indium in a cyclotron accelerator. *Journal of Nuclear Science and Technology.* 2024;**45**(1):99-106. doi: 10.24200/nst.2022.1217.1791.

24. Stokke C, Gnesin S, Tran-Gia J, Cicone F, Holm S, Cremonesi M, et al. EANM guidance document: dosimetry for first-in-human studies and early phase clinical trials. *Eur J Nucl Med Mol Imaging.* 2024;**51**(5):1268-86. doi: 10.1007/s00259-024-06640-x. PubMed PMID: 38366197. PubMed PMCID: PMC10957710.

25. Yousefnia H, Zolghadri S, Jalilian AR, Tajik M, Ghannadi-Maragheh M. Preliminary dosimetric evaluation of (166)Ho-TTHMP for human based on biodistribution data in rats. *Appl Radiat Isot.* 2014;**94**:260-5. doi: 10.1016/j.apradiso.2014.08.017. PubMed PMID: 25255303.

26. Han EY, Bolch WE, Eckerman KF. Revisions to the ORNL series of adult and pediatric computational phantoms for use with the MIRD schema. *Health Phys.* 2006;**90**(4):337-56. doi: 10.1097/01.HP.0000192318.13190.c4. PubMed PMID: 16538139.

27. Wang W, Cheng MY, Long PC, Hu LQ. Specific absorbed fractions of electrons and photons for Rad-HUMAN phantom using Monte Carlo method. *Chinese Phys C.* 2015;**39**(7):078203. doi: 10.1088/1674-1137/39/7/078203.

28. Sparks RB, Aydogan B. Comparison of the effectiveness of some common animal data scaling techniques in estimating human radiation dose. Oak Ridge Associated Universities, TN (United States); 1999.

29. Radfar E, Jalilian AR, Yousefnia H, Bahrami-Samani A, Ghannadi-Maragheh M. A comparative study of preliminary dosimetry for human based on distribution data in rats with 111In, 90Y, 153Sm, and 177Lu labeled rituximab. *Nuclear Technology and Radiation Protection.* 2012;**27**(2):144-51. doi: 10.2298/NTRP1202144R.

30. Snyder WS. "S" absorbed dose per unit cumulated activity for selected radionuclides and organs. MIRD Pamphlet no. 11. 1975. New York: Society of Nuclear Medicine; 1975.

31. Lahooti A, Shanehsazzadeh S, Jalilian AR, Tavakoli MB. Assessment of effective absorbed dose of (111)In-DTPA-Buserelin in human on the basis of biodistribution rat data. *Radiat Prot Dosimetry.* 2013;**154**(1):1-8. doi: 10.1093/rpd/ncs137. PubMed PMID: 22874898.

32. Vallabhajosula S, Kuji I, Hamacher KA, Konishi S,

Kostakoglu L, Kothari PA, et al. Pharmacokinetics and biodistribution of 111In- and 177Lu-labeled J591 antibody specific for prostate-specific membrane antigen: prediction of 90Y-J591 radiation dosimetry based on 111In or 177Lu? *J Nucl Med.* 2005;**46**(4):634-41. PubMed PMID: 15809486.

33. Cristy M, Eckerman KF. Specific Absorbed fractions of energy at various ages from internal photon sources. Report ORNL/TM-8381/V1–V7; TN (United States): Oak Ridge National Laboratory; 1987.

34. Stabin MG, Siegel JA. Physical models and dose factors for use in internal dose assessment. *Health Phys.* 2003;**85**(3):294-310. doi: 10.1097/00004032-200309000-00006. PubMed PMID: 12938720.

35. Ocampo JC, Puerta JA, Morales J. Evaluation of specific absorbed fractions from internal photon sources in the ICRP Reference Male Phantom. *Radiat Prot Dosimetry.* 2013;**157**(1):133-41. doi: 10.1093/rpd/nct124. PubMed PMID: 23704359.

36. Karimkhani S, Yousefnia H, Faghihi R, Gramifar P, Parishan MR. Calculation of Gallium-68 dose factors for [68Ga] DOTATATE injected patients: a comparison with OLINDA Database. *Journal of Nuclear Research and Applications.* 2022;**2**(2):30-40. doi: 1024200/jon.2022.1018.

37. Hermes Medical Solutions. Internal radionuclide dose calculation. Available from: https://www.hermesmedical.com/our-software/dosimetry/olinda/. 2024.

38. Demirci E, Toklu T, Yeyin N, Ocak M, Alan-Selcuk N, Araman A, Kabasakal L. Estimation of the organ absorbed doses and effective dose from 68Ga-PSMA-11 PET scan. *Radiat Prot Dosimetry.* 2018;**182**(4):518-24. doi: 10.1093/rpd/ncy111. PubMed PMID: 30137614.

39. Zhang J, Zhang J, Xu X, Lu L, Hu S, Liu C, et al. Evaluation of Radiation dosimetry of 99mTc-HYNIC-PSMA and imaging in prostate cancer. *Sci Rep.* 2020;**10**(1):4179. doi: 10.1038/s41598-020-61129-5. PubMed PMID: 32144340. PubMed PMCID: PMC7060171.

40. Khawar A, Eppard E, Sinnes JP, Roesch F, Ahmadzadehfar H, Kürpig S, et al. [44Sc]Sc-PSMA-617 Biodistribution and Dosimetry in Patients With Metastatic Castration-Resistant Prostate Carcinoma. *Clin Nucl Med.* 2018;**43**(5):323-30. doi: 10.1097/RLU.0000000000002003. PubMed PMID: 29485430.

41. International Atomic Energy Agency. Isotope Browser Software. Available from: https://play.google.com/store/apps/details?id=iaea.nds.nuclides&hl=en&pli=1. 2024.

42. Yousefnia H, Zolghadri S, Shanehsazzadeh S. Estimated human absorbed dose of ^{177}Lu-BPAMD based on mice data: Comparison with ^{177}Lu-EDTMP. *Appl Radiat Isot.* 2015;**104**:128-35. doi: 10.1016/j.apradiso.2015.06.033. PubMed PMID: 26163291.

43. ICRP. Radiological protection in biomedical research. ICRP Publication 62; 1992.